energies

MDPI

Article

Organic Geochemical Features of the Upper Paleozoic Coal-Bearing Deposits in Ordos Basin, North-Central China

Zonglin Li [1,2], Hong Li [1,2,*], Wenhou Li [1,2], Jiaopeng Sun [1,2] and Keyong Li [3]

[1] State Key Laboratory of Continental Dynamics, Northwest University, Xi'an 710069, China
[2] Department of Geology, Northwest University, Xi'an 710069, China
[3] College of Geology and Environment, Xi'an University of Science and Technology, Xi'an 710054, China
* Correspondence: lihong2008@nwu.edu.cn

Abstract: The exploration of hydrocarbon resources plays a critical role in fulfilling the world's increasing demand for energy. In this regard, the distribution and source rock characteristics of coal measure stratum in the whole basin are important and must be studied. However, systematic research has not been conducted yet. In this study, organic geochemical data, drilling data, and fieldwork were used to examine the source rock distribution of the Upper Paleozoic stratum. The results revealed that Upper Paleozoic coal-bearing rock series are mostly present in the Benxi, Taiyuan, and Shanxi formations, and mudstones and coals are formed frequently in tidal flat deposits. The layers of the coal and mudstone are primarily thick on the western sides, eastern sides, and northern sides, thin in the middle region, and gradually thinner from north to south. The source rocks are mostly enriched in the east and west of the basin. The results of the Rock-Eval pyrolysis analysis indicated that the overwhelming majority of the coal comprises excellent source rocks, all limestones are poor source rocks, and most mudstones are good–excellent source rocks. The kerogen type of most of the rock samples is type III, suggesting typical "gas source" kerogen. Humus is derived from terrestrial organism and aquatic algae remnants, indicating a diversified parent material input. These results evidence that studied source rocks are at the postmature-dry gas stage.

Keywords: source rocks; organic matter accumulation; coal-bearing stratum; Upper Paleozoic; Ordos Basin

check for updates

Citation: Li, Z.; Li, H.; Li, W.; Sun, J.; Li, K. Organic Geochemical Features of the Upper Paleozoic Coal-Bearing Deposits in Ordos Basin, North-Central China. *Energies* **2023**, *16*, 2302. https://doi.org/10.3390/en16052302

Academic Editor: Renato Somma

Received: 14 December 2022
Revised: 4 February 2023
Accepted: 24 February 2023
Published: 27 February 2023

Copyright: © 2023 by the authors. Licensee MDPI, Basel, Switzerland. This article is an open access article distributed under the terms and conditions of the Creative Commons Attribution (CC BY) license (https://creativecommons.org/licenses/by/4.0/).

1. Introduction

Ordos Basin, the submaximal petroliferous basin in China, is a multicycle, inland, cratonic, and petroliferous one with stable subsidence and depression migration, has abundant natural gas resources, and boasts huge potential [1–3]. The total amount of petroleum resources in the basin is 15.2×10^{12} m^3, with recoverable resources of 8.93×10^{12} m^3. Following more than 60 years of hydrocarbon resource exploration in Ordos Basin, large-scale gas fields known as the Sulige, Daniudi, Yulin, Shenmu fields have been prospected [4–6]. Furthermore, the Ordos Basin is saturated by wealthy unconventional hydrocarbon resources [7]. By the end of 2018, 72 large gas fields were found in China, with total explored geological reserves of 12.5×10^{12} m^3, of which the explored geological reserves of 12 large gas fields in the Upper Paleozoic of Ordos Basin accounted for nearly a third [8]. Ordos Basin is a typical block of large lithologic gas reservoir distribution in China [9,10]. According to current research, Carboniferous–Permian biogenic limestones, dark mudstones, and coal seams are widely regarded as hydrocarbon source rocks in the whole basin (Figure 1). The main source rocks are coal rocks, followed by dark mudstones, and biological limestones contribute the least. Additionally, it is believed that Benxi Formation, Taiyuan Formation, and Shanxi Formation are the principal gas-producing positions of Upper Paleozoic hydrocarbon source rocks. However, Shihezi Formation and Shiqianfeng Formation mudstones are mostly non-hydrocarbon source rocks. An analysis concerning the characteristics of source beds in the Upper Paleozoic coal-measure strata is helpful in

enriching the geological theory behind natural gas accumulation, and it holds considerable reference value for hydrocarbon resource exploration in the basin and in larger areas in the future.

2. Geologic Setting

Located in the western margin (34°00′~41°20′ N, 105°30′~110°30′ E) of the North China Craton, the Ordos Basin is a large multicycle cratonic basin, and the most stable block (Figure 2a) [11,12] spaces cover up to 25×10^4 km^2 [13]. In the regional tectonic unit, the west of the basin is bounded by the Helan fault fold belt and the Liupanshan arc thrust belt, and it is adjacent to the Alaxa block; the north is bordered on the Ancient Yinshan fold orogenic belt by the Yimeng uplift; the east is bounded by the Yishan block; the southwest margin is bounded by the Qilian–Qinling Orogenic system [11,12,14]. Given the current tectonic features, evolutionary history, tectonic development, and tectonic characteristics of the Ordos Basin, it has been divided into six structural units shown as Figure 2b [15–17]. This tectonic framework was formed during the Yanshan Orogenic period, developing and being completed during the Himalayan Orogenic period [18,19]. The Ordos Basin has experienced many multi-episodic tectonic orogenies in its long geological history [20,21], which has led to the basin-filling evolution characteristics of abundant sediment types, a clear structural cycle, and various sequence stratum types in the Upper Paleozoic sedimentary of basin. In the late Early Paleozoic, the north–south ocean basin was in the period of arc–continent collision [22–24]. Following the Middle Ordovician, the North China plate was uplifted, long-term weathered, and denuded [25]. Since the beginning of the Late Paleozoic, the Ancient Qilian–Qinling Block and the North China Block collided, causing the overall uplift of the paleorift continental margin in the Ordos area [26,27]. Moreover, since the Late Carboniferous, because of the east–west extension, the platform had subsided as a whole, and the Tianshan Orogeny in the Late Carboniferous caused the southward subduction of the Xingmeng trough [28]. The Indosinian Orogeny began in the Late Permian and caused the northward subduction of the Qinling Ocean trough, and the tectonic pattern of these areas changed [29]. Multiple orogenies led to the extensive development of marine–terrestrial interactive rocks in the Paleozoic of the basin [30].

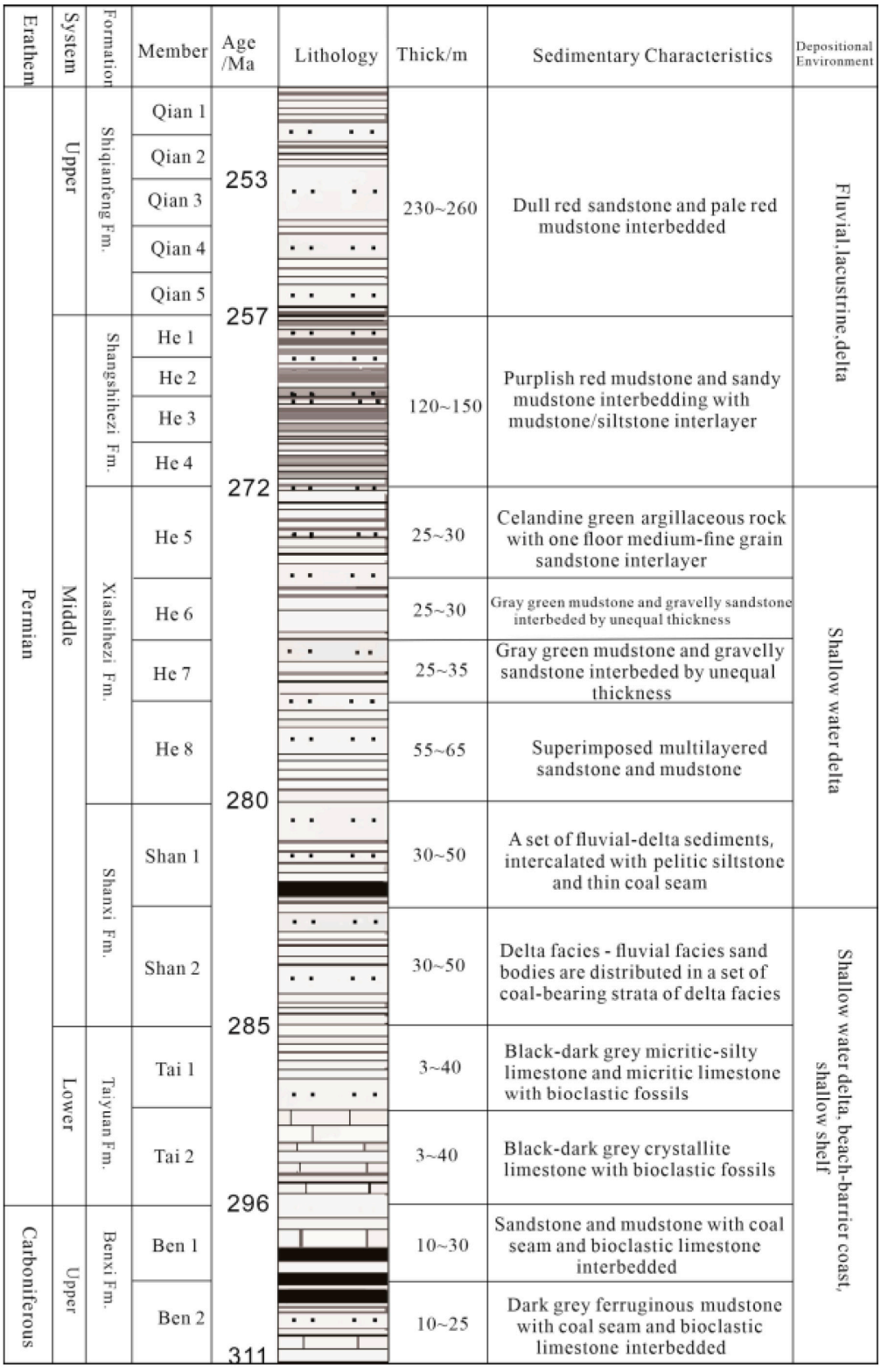

Figure 1. A comprehensive stratigraphic histogram of Upper Paleozoic strata in the Ordos basin.

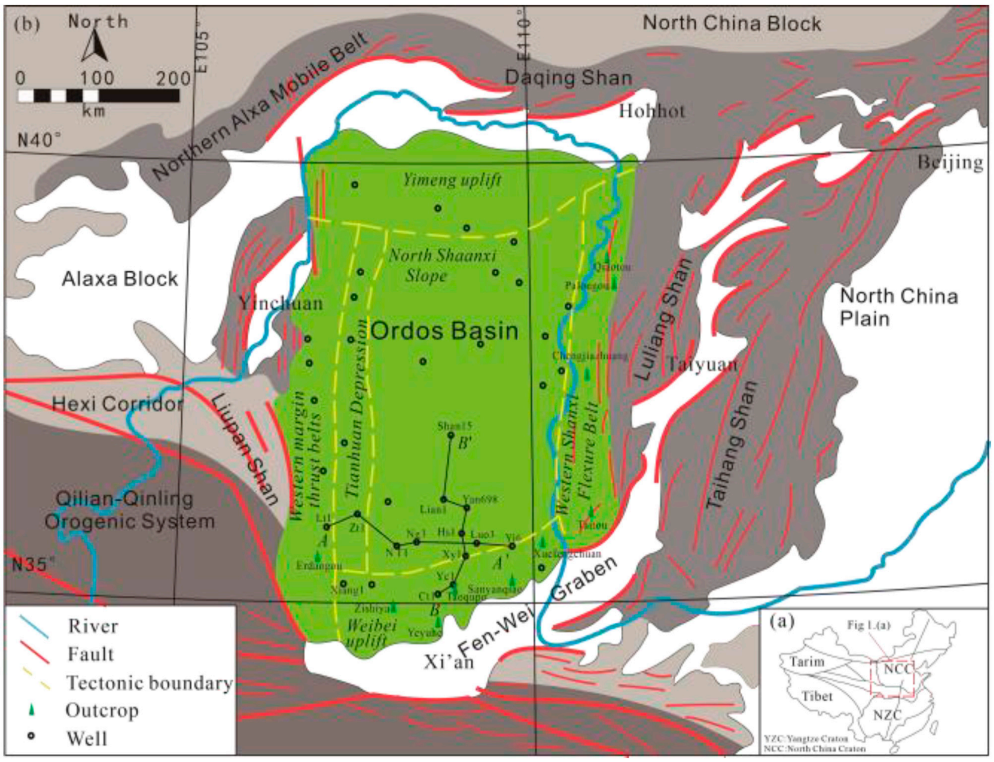

Figure 2. (**a**) Location of the Ordos basin in China. (**b**) Tectonic division and location of sampling wells, outcrops, and cross-sections in the Ordos Basin. (Adapted from Ref. [10]).

3. Samples and Methods

3.1. Sample Selection

In total, 132 rock samples from the Benxi, Taiyuan, and Shanxi formations were collected from 38 wells in the Ordos Basin (Figure 2). These samples comprised 96 mudstones, 24 coals, and 12 limestones. The rock samples were washed with distilled water and, then, dried at 25 °C. Each dry sample is ground to 200 mesh and weighed 15 g for subsequent measurement.

3.2. Rock-Eval Analysis

Rock pyrolysis was performed on the 132 rock samples using a Rock-Eval VI instrument in an oil and gas evaluation workstation in the State Key Laboratory of Continental Dynamics, Northwest University. Weigh 30–50 mg of powder for each sample, and the weighed samples were then transferred in the Rock-Eval VI to pyrolysis. Peters and Cassa [31] and Behar et al. [32] provided the specific procedures, technical standards, and parameter explanation of the experiment.

3.3. Total Organic Carbon Content (TOC) Measurement

The TOC contents of 132 samples were measured by the Leco CS744 analyzer of the State Key Laboratory of Continental Dynamics, Northwest University. Dissolve the rock sample in 12.5% HCl for at least 2 h, remove the carbonate after heating (80 °C), water washing, filtering, and then dry it at 80 °C after removing the chloride ion. After that, burn the organic carbon into CO_2 gas in the high-temperature oxygen flow (2.4×10^5 Pa). The content of organic carbon is obtained through infrared detector detection and computer calculation [33,34].

4. Stratigraphy Characteristics

The Upper Paleozoic source rocks in Ordos Basin are mostly marine–terrestrial interactive coal-bearing systems characterized by a wide superimposed pattern of coal-bearing source rocks, wide distribution of coal rocks and mudstones, and dense sandstone

reservoirs. The coal-bearing rock series are mainly in the Benxi, Taiyuan, and Shanxi formations [19–25].

4.1. Petrological Characteristics

Through 11 field outcrops, the source rocks mainly comprise dark mudstone, dark argillaceous limestone, and black coal. The dark mudstones have a uniform color, great brittleness, and poor plasticity. This strata is formed in a quiet water-reduction environment with ancient fossils inside. Coal layered in the strata is lightweight and brittle and has obvious glass luster [35–37].

The Benxi Formation is the sediment of the Ordos Basin in the early Late Paleozoic, which was formed by the southeastern transgression of the northern China Sea in the Variscan orogeny. Owing to the deposited Caledonian Ordovician erosional landform, the Benxi Formation evolved in the lower concave parts of the erosional landform in the form of fillings. The sediments include littoral clasolite, tidal flat limestone, littoral marsh facies coal, and carbonaceous mudstone (Figure 3a,b). The Taiyuan Formation was continuously deposited on the Benxi Formation. The sedimentary environment was controlled by tidal flat, and littoral-neritic sea The sediments were characterized by a series of interactive delta plain facies—tidal flat facies mudstone, carbonaceous mudstone, limestone, and coal seam (Figure 3c–e). The Ordos Basin stepped into a new evolutionary stage of offshore interior depression in the early Permian: a set of positive cyclic sedimentary sequences of continental delta front facies—distributary interchannel swamp facies—and lacustrine facies in the Shanxi Formation were characterized by gray-black mudstone, siltstone, medium-fine sandstone, and lower middle sandstone–coal seam components (Figure 3f).

4.2. Thickness of the Source Rock

The coal measure source rocks' thickness data was counted, and plane contour map of coal-bearing source rocks was drawn, including the thickness contour map of coal seam and mudstone in the Upper Paleozoic (Figure 4). The map shows that the source rock is present almost throughout the Ordos Basin and has the characteristics of wide plane distribution and large thickness variation.

The coal thickness is featured as mainly thick on the eastern and western sides, thin in the middle, thick in the north, and gradually thinner from north to south. Western high-value areas are gathered around Tianshuibao, Jiyuan, and Huanxian in the western basin, and the thickest part reaches 14 m, gradually thinning to match the surroundings. Midland high-value areas are gathered around Uxin Banner and Sulige (6–10 m) and compared to the side regions, which are not thick and less distributed. The thickest coal (greater than 20 m) in the northern basin focuses on the Jungar Banner, Shenmu, and Baode regions, and it gradually thins from north to south. In the south of the basin, the coal thickness in the Yichuan and Hejin regions is greater than 10 m.

Dark mudstones are also widely distributed in the coal measure strata of basin, which generally resembles coal's feature. The thicknesses of mudstones are ~100–120, ~60–70, and ~80–110 m in the east, middle, and west, respectively. Generally, the mudstones are thin in the middle basin and thick on the western and eastern sides.

4.3. Stratigraphic Distribution

W-E cross-section A-A′ and N-S cross-section B-B′ evince the stratigraphic characteristics. The locations of these outcrops are shown in Figure 2. An examination of the cross-sections (Figure 5) in different directions reveals that the Benxi Formation source rocks are characterized by thick middle and thin edge mudstone and western and eastern thick, but small, parts of the coal seam. The Taiyuan Formation's source rocks consist of lower middle marine mudstone facies, northern limestones, and upper large thick coal seams. The Lower Shanxi Formation's thick mudstone alternates with thick siltstone. Moreover, the middle areas show the thick coal seam gradually pinching out on both sides and a wide extension of the thin coal seam in the Shanxi Formation.

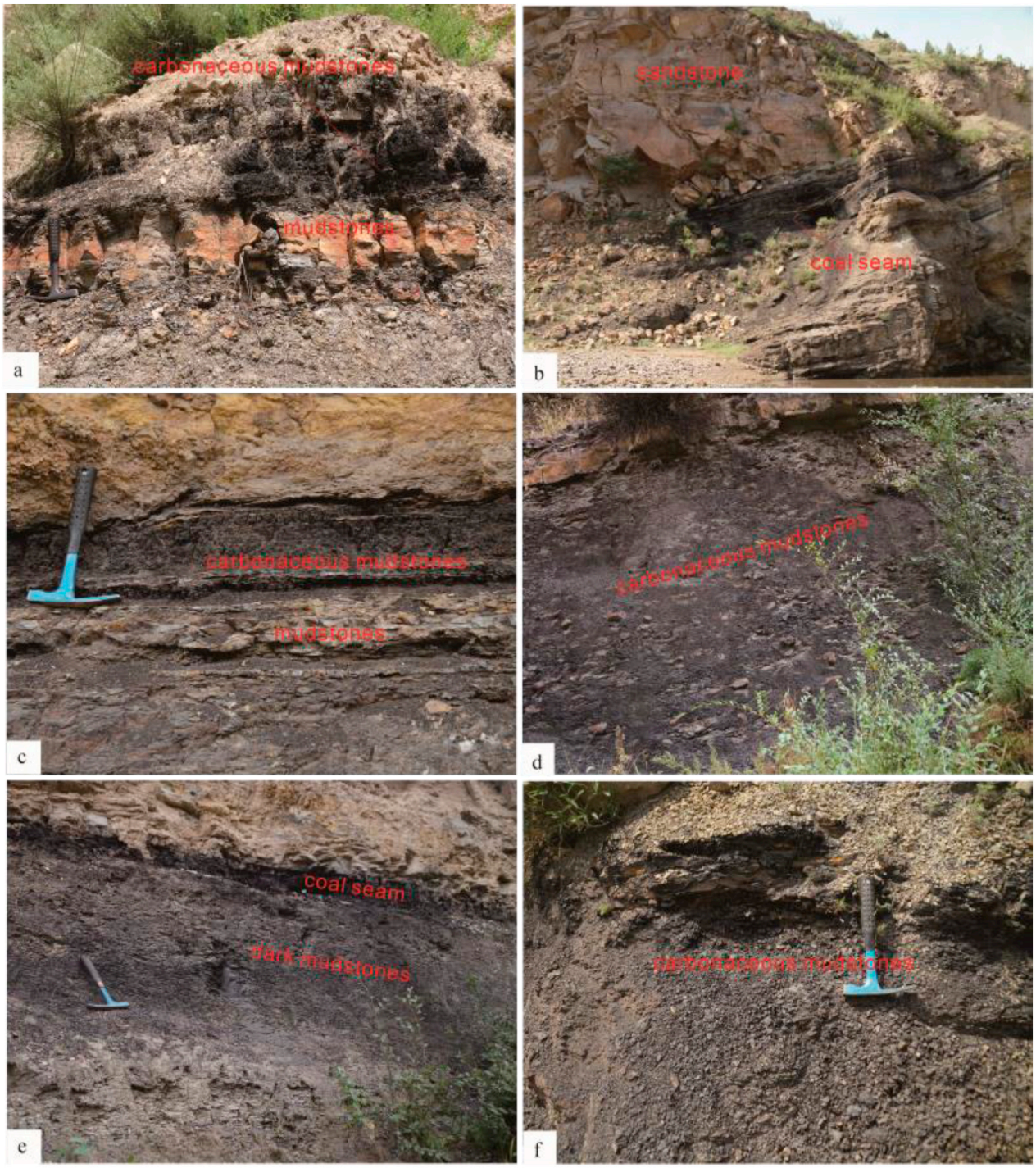

Figure 3. Photographs showing the lithofacies association and typical sedimentary characteristic in the Upper Paleozoic source rocks in the Ordos Basin. (**a**) Benxi Formation carbonaceous mudstones of the peat flat of the tidal flat in the Guanjiaya Section; (**b**) Benxi Formation coal seam of the mud flat of tidal flat facies in the Qiaotou Section; (**c**) Taiyuan Formation carbonaceous mudstones of the peat flat of the tidal flat in the Sanyanqiao Section; (**d**) Taiyuan Formation carbonaceous mudstones of the mud flat of the tidal flat in the Palougou Section; (**e**) Taiyuan Formation coal seams and carbonaceous mudstones of the mud flat of the tidal flat in the Guanjiaya Section; (**f**) Shanxi Formation carbonaceous mudstones of the tidal flat in the Xuefengchuan Section. The locations of these outcrops are shown in Figure 2.

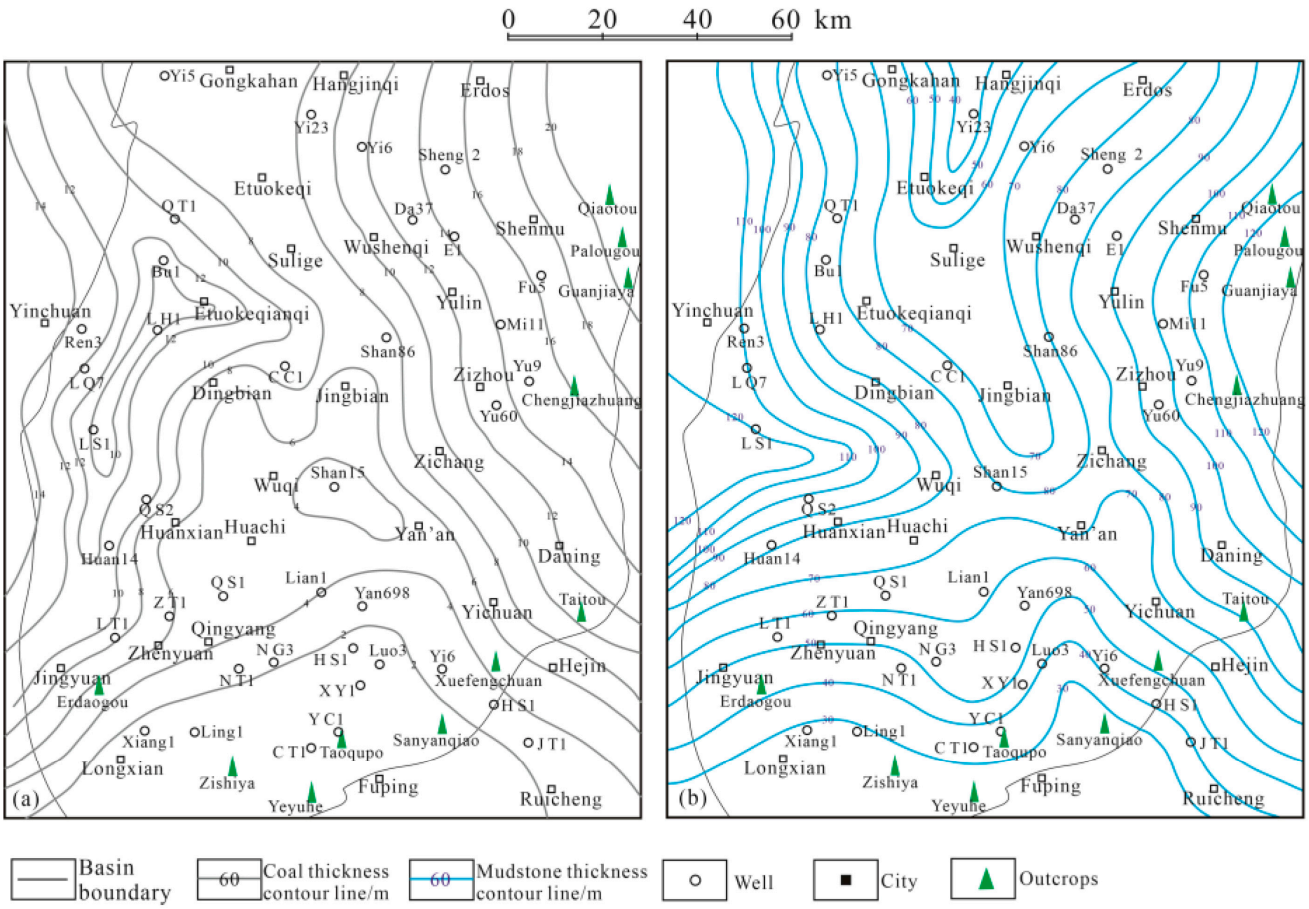

Figure 4. Distribution of the Upper Paleozoic coal measure source rocks in the Ordos Basin.

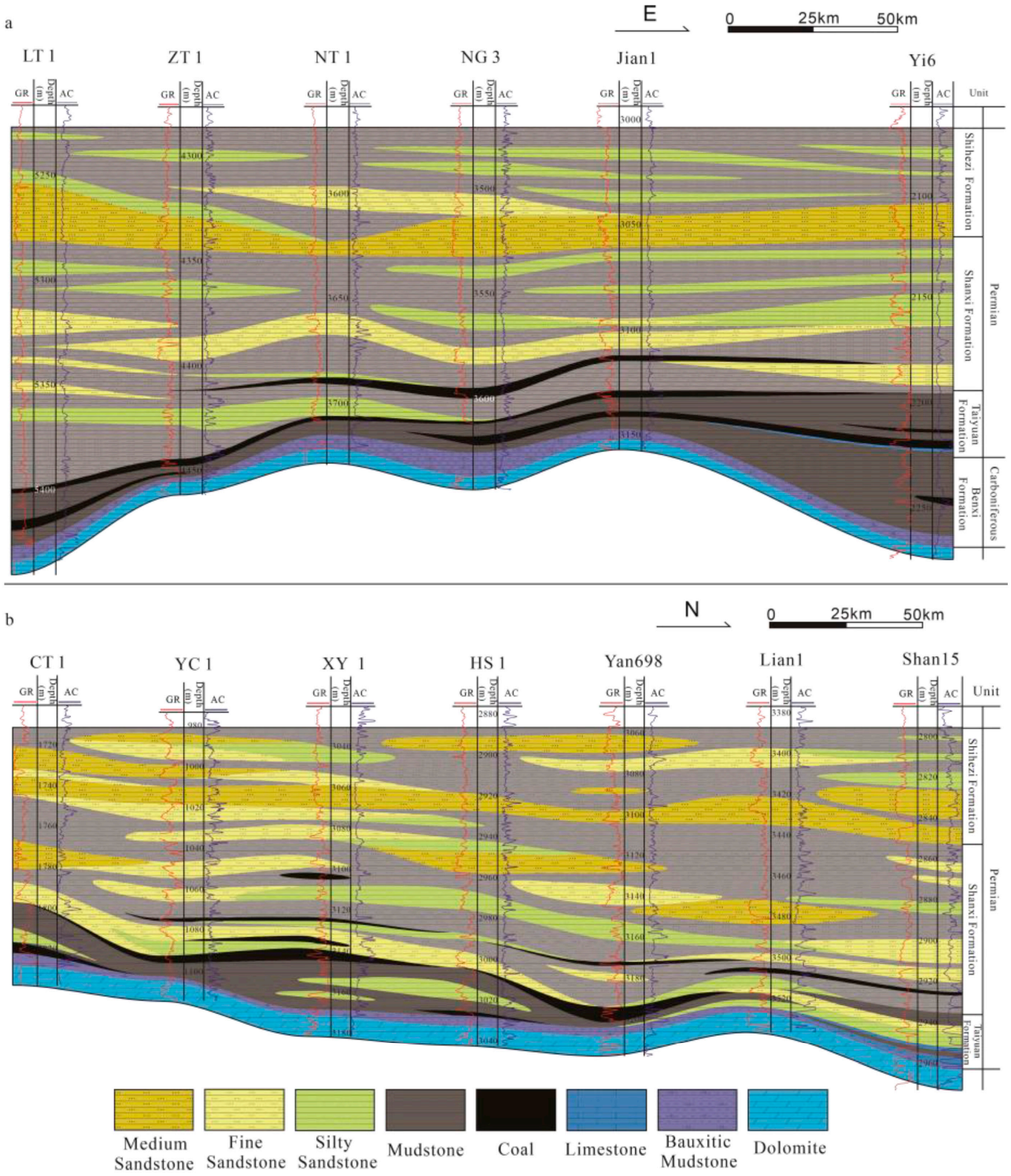

Figure 5. Schematic geological sections of the Upper Palezoic rocks in the Ordos Basin (**a**). Schematic geological section of A—A′ cross-section; (**b**). Schematic geological section of B—B′ cross-section. A—A′ cross-section connected by LT1—ZT1—NT1—NG3—Jian1—Yi6; B—B′ cross-section connected by CT1—YC1—XY1—HS1—Yan698—Lian1—Shan15). The locations of these wells are shown in Figure 2. SP: wireline logging of the spontaneous potential; GR: wireline logging of the natural gamma response.

5. Organic Geochemical Characteristics

5.1. Total Organic Matter Content (TOC)

TOC and (S1 + S2), generally used measures to assess the quantity of organic matter in studied samples [31,38,39], were calculated. Using the S1 plus S2 values, the potential yield, alternate name genetic potential, is obtained from rock evaporation pyrolysis. S1, the volume of hydrocarbon in the source rock, has been formed by the maturity and removed from the rock during pyrolysis. S2 refers to the bitumen produced by consecutive burial and maturation before finishing, which reduces with maturity [31].

The 26 members of the Upper Paleozoic have coal TOC values from 8.88 to 97.16 wt% (44.92 wt%, on average), the 109 members have mudstone TOC values from 0.01 to 8.87 wt% (1.69 wt%, on average), and the 17 members have limestone TOC values from 0.04 to 2.20 wt% (0.41 wt%, on average). The S1 + S2 values of the coals ranged from 0.18 to 29.04 mg HC/g rock (6.62 mg HC/g, on average), those of the mudstones were 0.02 to 4.10 mg HC/g rock (0.21 mg HC/g, on average), and those of the limestones were in the range of 0.02 to 0.54 mg HC/g rock (0.08 mg HC/g, on average) (Table 1). According to the standard of source rocks referred to by Peters and Cassa [20], the TOC and S1 + S2 contents indicate that the overwhelming majority of coals are excellent source rocks, and the majority of limestones are poor source rocks, while mudstones have a large difference in TOC and S1 + S2 contents, which warrants further study.

Table 1. Rock-Eval pyrolysis data of the source rock samples.

System	Samples	TOC (%)	T_{max} (°C)	S1 (mg/g)	S2 (mg/g)	S1 + S2	HI (mg/g)	R_O (%)
Upper Paleozoic	Coals	8.88~97.16	503~592	0.01~1.58	0.16~27.61	0.18~29.04	1.00~41.12	1.99~2.82
		44.92	549	0.32	6.01	6.62	12.77	2.38
	Mudstones	0.01~8.87	269~589	0.01~0.41	0.01~3.70	0.02~4.10	1~1000	1.59~2.62
		1.69	512	0.02	0.21%	0.21	731	2.25
	Limestones	0.04~2.20	370~566	0.01~0.54	0.01~0.54	0.02~0.54	2~140	2.05~2.91
		0.41	466	0.08	0.08	0.08	27.7	2.48
Upper Paleozoic	Benxi Formation mudstones	6.01~14.23	544~568	0.01~0.04	0.04~0.74	0.05~0.78	1.00~8.00	1.98~2.46
		9.14	561	0.01	0.36	0.37	4.00	2.26
	Taiyuan Formation mudstones	4.62~8.87	542~588	0.01~0.05	0.09~0.43	0.09~0.45	1.00~4.89	2.44~2.47
		6.84	568	0.02	0.18	0.22	2.46	2.46
	Shanxi Formation mudstones	0.01~6.63	269~589	0.01~0.04	0.01~3.70	0.01~3.72	2.00~1000.00	1.59~2.62
		1.04	506	0.02	0.20	0.22	81.20	2.24

TOC: Total organic carbon (mass percentage); S1: free hydrocarbon percentage; S2: residual petroleum potential; HI: hydrogen index; T_{max}: the temperature corresponding to the maximum hydrocarbon content (the highest value of S2) produced by the kerogen; R_O: reflectance of vitrinite. The data above the horizontal line in the table mean"minimum value~maximum value", and the data below the horizontal line means "average value", the data in brackets mean sample quantity.

The TOC vs. S1 + S2 plot shows that all the mudstones of the Benxi Formation and Taiyuan Formation are excellent source rocks, but only 37.2% of the Shanxi Formation mudstones are good–excellent source rocks. All the Benxi Formation and Taiyuan Formation mudstones are in an adequate gas region, as shown in the plot of HI versus TOC (Figure 6b). A portion (34.9%) of the Shanxi Formation mudstones shows affluent petroleum potential, and minor samples (2.3%) are in a good oil generation region.

In addition, the S1 vs. TOC plot is always used to discriminate between allochthonous and autochthonous hydrocarbons [40]. It is known that the existence of migrated oil in source rocks can be found out by a high S1 and TOC. This correlation demonstrates that for all the studied rock samples of the coal, mudstone, and limestone members of the Benxi, Taiyuan, and Shanxi formations, the results show that most samples belong to the autochthonous hydrocarbons region, showing that the petroleum was generated in the source rock itself (Figure 6c).

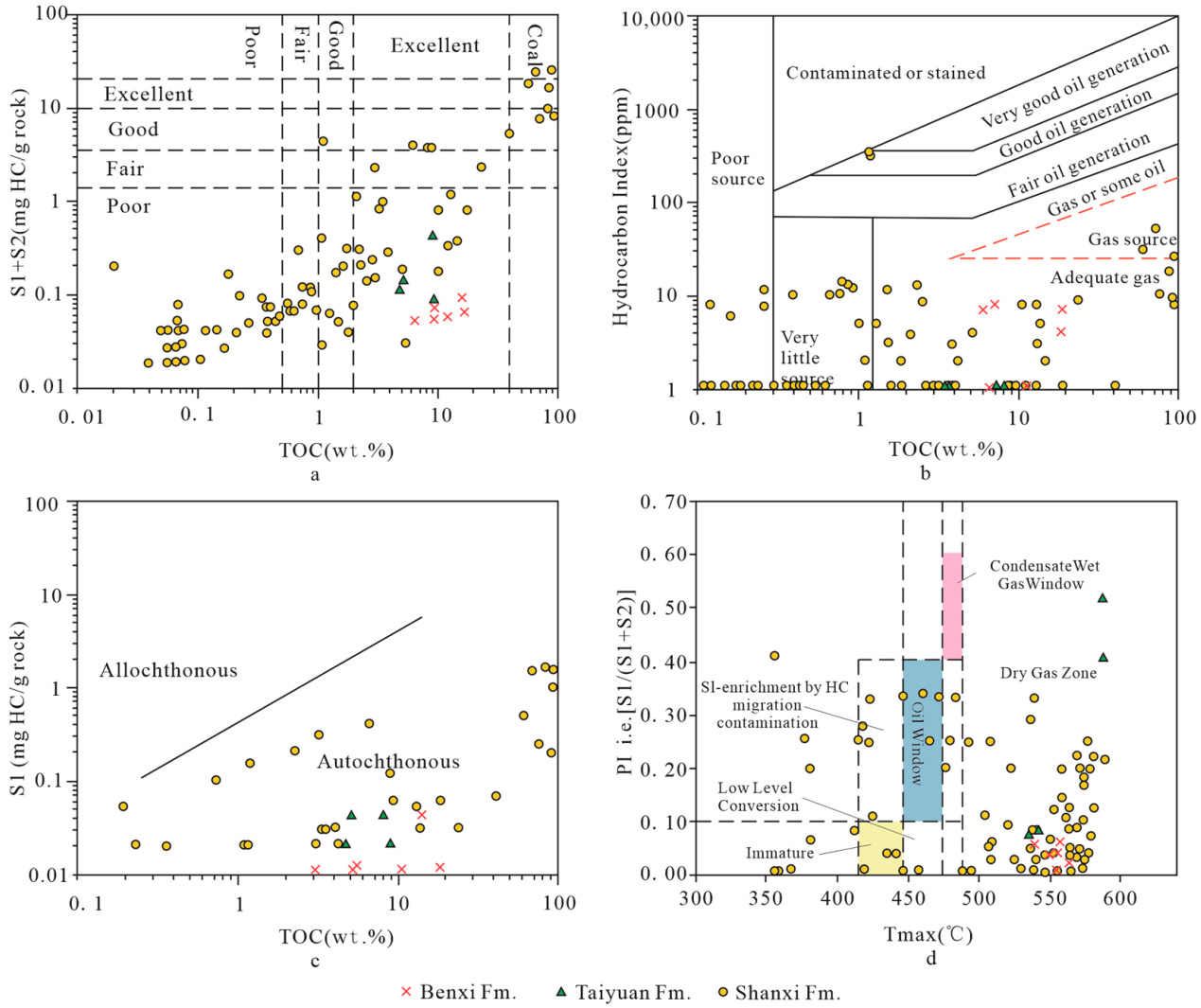

Figure 6. Cross-plots: (**a**) the wax indexes versus TOC/S1 + S2; (**b**) the wax indexes versus TOC/hydrocarbon index; (**c**) the wax indexes versus TOC/S1; (**d**) the wax indexes versus Tmax/PI [S1/(S1 + S2)].

The variations in TOC isoline along the longitudinal and horizontal directions are illustrated in Figure 7. The TOC values in this area are generally higher in the southern basin and lower in the northern basin. Except for the Jingyuan and Longxian regions, most areas belong to good–excellent source rocks (TOC > 0.5%); the values exceed 3.0% in the middle and eastern Ordos Basin.

5.2. Genetic Type of Kerogen

The quality of source rocks can be evaluated not only using TOC and Rock-Eval pyrolysis but also by the genetic type of kerogen, which hinges on the origin of source rock and the corresponding maceral composition [31,39,41–45].

Kerogen has been divided into three categories: namely, type I (algae or bacterial modification), type II (originate from marine plankton and microorganisms), and type III (continental higher plants) [46]. Type II kerogen has been further classified into type II1 and type II2 for continental source rocks [46]. From the results of the maceral composition (Table 2), the kerogens belong to type II1, type II2, and type III. Among them, the vitrinite compositions of most coals exceed 90%, corresponding to type III. The kerogens of most limestones and mudstones are also type III, suggesting a typical "gas source" kerogen. It is indicated that vitrinite is the highest in maceral composition of coal (69.23%~100%),

followed by exinite (0~30.77%), which is rich in hydrogen and stable. Meanwhile, the maceral composition of Upper Paleozoic mudstone's type III kerogens is similar to that of coal, which is mainly vitrinite, with low exinite and inertinite content. Plus, maceral composition of Type II1 kerogens is dominated by exinite, the minority is made up of vitrinite, and that of type II2 kerogen is characterized by low inertinite, with Sapropelinite, Exinite, and Vitrinite occupying a certain proportion, respectively. Moreover, the sapropelinite in some mudstones is slightly higher, revealing that humus is derived not only from terrestrial organism remnants but also from a few aquatic algae remnants because of different sediments. Overall, the parent material input of the Upper Paleozoic source rocks is derived from diversified organisms.

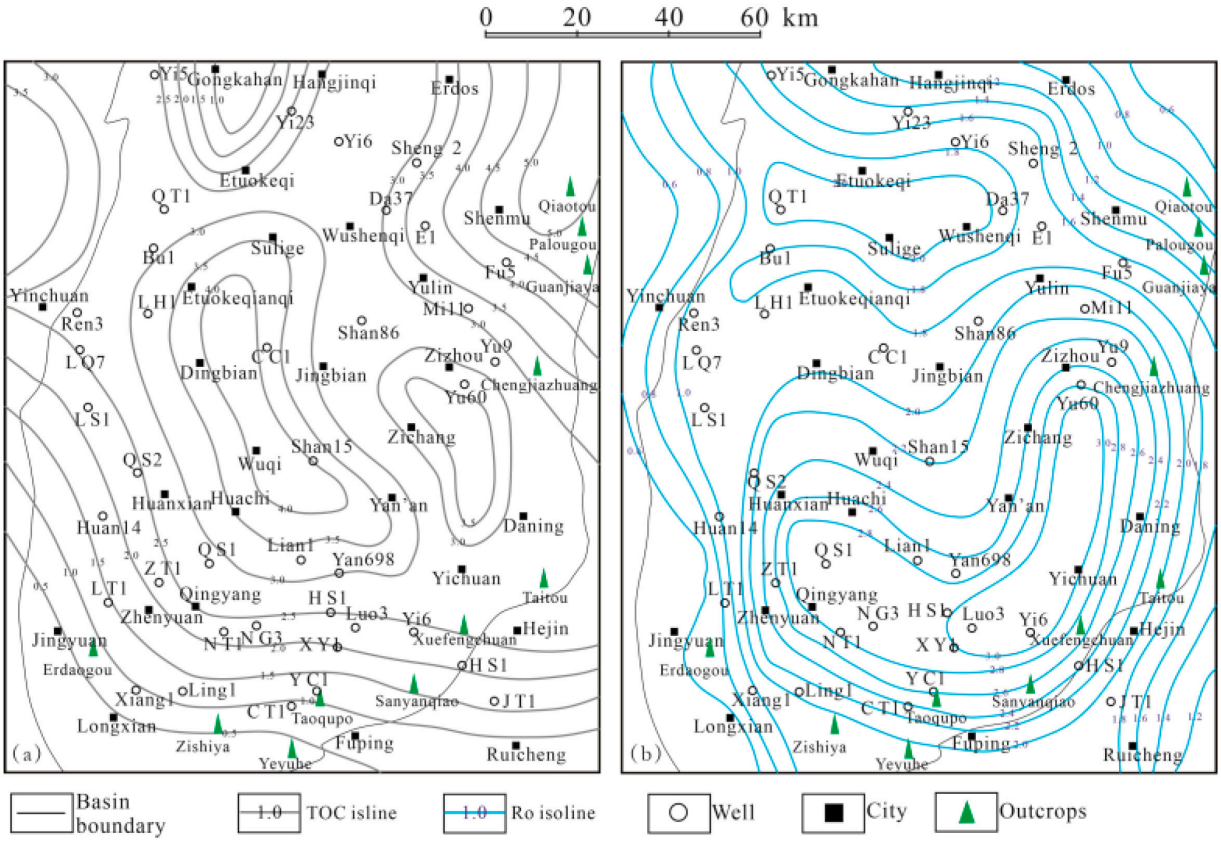

Figure 7. Features of TOC and thermal evolution of source rocks in the Ordos Basin. (a. TOC isoline of source rocks in the Ordos Basin; b. R_0 isoline of source rocks in the Ordos Basin.)

5.3. Stage of Thermal Maturation

Both thermal maturation and compositions of organic matter are the pivotal influencing factors that decide the distribution and consistency of organic substance discharged from source rocks. The T_{max} vs. PI plot determines that the hydrocarbons of the rock samples are mostly nonindigenous affiliated to gas [47]. In this study, all of the T_{max} (°C) values, from diverse formations of the Upper Paleozoic, range from 269 °C to 592 °C, together, with inequable PI values (Figure 6d). By reason of all the Benxi and Taiyuan, as well as most of the Shanxi formation mudstones, being in the dry gas region, as shown in Figure 6d, the Upper Paleozoic source rocks are at the postmature-dry gas stage. The T_{max} is improved gradually with maturation and can be interrelated with vitrinite reflectance, so R_O can be estimated from the T_{max} values obtained from the Rock-Eval pyrolysis [39,41]. According to calculated R_O, on the HI vs. R_O plot, the majority of the samples fall into the dry gas window region shown in Figure 8, the result is consistent with the study above.

Table 2. Maceral compositions (%) and kerogen types for the source rock samples.

System	Samples	Sapropelinite (%)	Exinite (%)	Vitrinite (%)	Inertinite (%)	Kerogen Type
Upper Paleozoic	Coals	0	0~30.77% 8.16(24)	69.23%~100% 91.84%(24)	0	III
	Limestones	12.77%~36.25% 23.66%(7)	0.26%~2.45% 0.88%(7)	45.66%~85.14% 74.03%(7)	0.88%~2.20% 1.43%(7)	III
		60.98%~80.13% 66.93%(5)	16.21%~24.65% 19.71%(5)	8.99%~19.45% 13.36%(5)	0	II_2
Upper Paleozoic	Benxi Formation mudstones	68.37%~78.81% 73.19%(3)	16.66%~21.49% 18.27%(3)	6.80%~13.93% 10.50%(3)	0	II_2
		2.70%~8.81% 3.39%(3)	49.34%~65.94% 58.98%(3)	7.53%~13.64% 10.99%(3)	0	II_1
	Taiyuan Formation mudstone	0	29.43%~36.88% 31.85%(4)	50.06%~75.61% 58.33%(4)	7.91%~13.49% 9.82%(4)	III
	Shanxi Formation mudstone	0~40.30% 19.50%(58)	0~43.5% 7.28%(58)	48.58%~98.12% 63.76%(58)	0~42.21% 9.46%(58)	III
		0~69.30% 28.80%(25)	16.69~84.87% 39.14%(25)	15.13%~76.72% 31.82%(25)	0~1.30% 0.24%(25)	II_2
		0	88.19~96.47% 94.23%(3)	6.64%~8.37% 5.77%(3)	0	II_1

The data above the horizontal line in the table mean"minimum value~maximum value", and the data below the horizontal line means "average value", the data in brackets mean sample quantity.

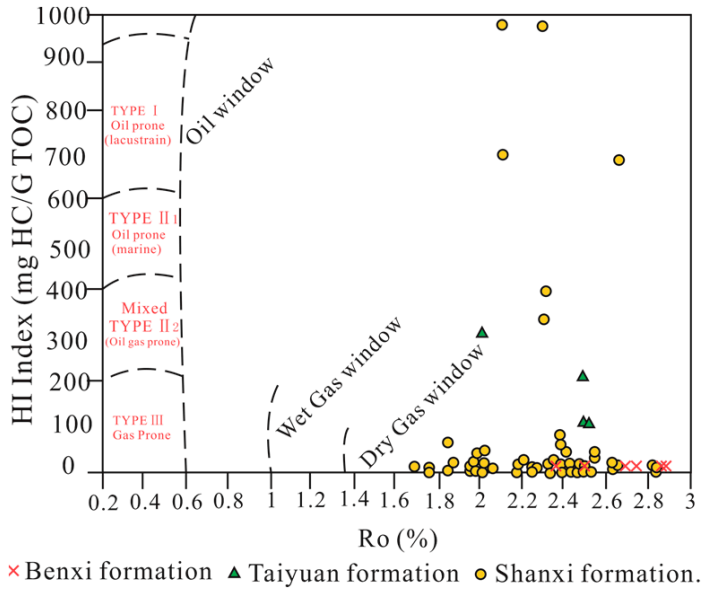

Figure 8. A plot of HI versus R_O displaying the type and maturity of samples.

Variations of calculated vitrinite reflectance isoline, along longitudinal and horizontal directions, are regular by the thermal evolution of the Fuxian and Yanchang regions (R_O > 3.0%), while in the south, they are relatively high and gradually reduce to the surrounding values shown in Figure 7. The values of R_O in this area generally reached the postmature-dry gas stage (R_O > 2.0%). It is worth mentioning that variations of thermal evolution and TOC showed a contrary trend of the thickness to mudstones and coals, which suggest that the thickness of source rock is not directly correlated to hydrocarbon generation potential.

5.4. Comprehensive Evaluation

Coals and mudstones from the Upper Paleozoic are developed in the eastern and western parts of the basin, which are the main distribution areas of hydrocarbon source rocks. In addition, the relatively high TOC values (on average, 44.92%) mean that it is greatly conducive to the generation of natural gas, which is the main gas source rock of the Upper Paleozoic natural gas in the region. Plus, the average organic carbon content of dark mudstones is 1.69%, indicating a relatively strong capacity of hydrocarbon generation, and its supply capacity for natural gas is only less than that of coal. Moreover, Rock-Eval data shows that most of samples studied behave as if they have reached the dry gas stage and are regarded as the good–excellent source rocks. The main types of kerogens in the studied Upper Paleozoic source rocks are type II1, type II2 and type III kerogens. In summary, the Upper Paleozoic coals and mudstones have high hydrocarbon generation potential and exploitation value.

6. Conclusions

From the systematic analysis of the bulk sedimentary and organic geochemical characteristics associated with the Upper Paleozoic source rocks, the following conclusions can be reached:

(1) The Upper Paleozoic coal-bearing rock series are present, mainly, in the Benxi, Taiyuan, and Shanxi formations. Mudstones and coals are formed frequently in tidal flat deposits. The thickness distribution of coal and mudstone is as follows: thick in the east, north, and west basin, thin in the middle, and gradually thinner from north to south. The thick source rocks are mostly enriched in the eastern and western Ordos Basin.

(2) The results of the Rock-Eval pyrolysis indicate that the overwhelming majority of coals are excellent source rocks, all the limestones are poor source rocks, and most of the mudstones are good–excellent source rocks. The kerogens of most of the rock samples are of type III, suggesting a typical gas source kerogen. Humus is derived from terrestrial organism and aquatic algae remnants, indicating diverse parent materials. It is evident from these results that the Upper Paleozoic source rocks are at the postmature-dry gas stage.

Author Contributions: Conceptualization, Z.L., H.L. and W.L.; methodology, K.L. and J.S.; formal analysis, Z.L., W.L. and K.L.; investigation, Z.L., J.S. and W.L.; data curation, Z.L. and K.L.; writing-original draft preparation, Z.L. and K.L.; writing- review and editing, Z.L., H.L. and J.S.; supervision, W.L.; funding acquisition, H.L. All authors have read and agreed to the published version of the manuscript.

Funding: This research was funded by the National Natural Science Foundation of China, grant number 41272115, 41572086.

Data Availability Statement: Not applicable.

Conflicts of Interest: The authors declare no conflict of interest.

References

1. Liu, J.; Liu, K.; Liu, C. Quantitative evaluation of gas generation from the Upper Paleozoic coal, mudstone and limestone source rocks in the Ordos Basin. *China. J. Asian Earth Sci.* **2019**, *178*, 224–241. [CrossRef]
2. Wang, W.F.; Liu, P.; Zheng, L.; Zhou, X.G.; Jiang, S. Natural gas reserves and production prediction of Ordos Basin. *Nat. Gas Geosci.* **2014**, *25*, 1483–1490, (In Chinese with English abstract).
3. Zhang, Y.; Jiang, S.; He, Z.; Wang, Y.; Guo, M.; Zhu, G.; Cai, D.; Lu, S.; Xiao, D.; Li, Y.; et al. Characteristics of heterogeneous diagenesis and modification to physical properties of Upper Paleozoic tight gas reservoir in eastern Ordos Basin. *J. Pet. Sci. Eng.* **2022**, *208*, 109243. [CrossRef]
4. Fu, J.H.; Fan, L.Y.; Liu, X.S.; Hu, X.Y.; Li, J.H.; Ji, H.K. New progresses, prospects and countermeasures of natural gas exploration in the Ordos Basin. *China Pet. Explor.* **2019**, *24*, 418–430, (In Chinese with English abstract).
5. He, F.Q.; Zhang, Y.; Wang, F.B.; Zhang, R.; Zhang, W.; Qi, R.; An, C.; Li, X.W.; Deng, J. Petroleum exploration progress and new field of Sinopec in Ordos Basin during the 13th Five-Year Plan period. *China Pet. Explor.* **2022**, *27*, 1–12, (In Chinese with English abstract).

6. Wang, G.N. Characteristics of upper paleozoic source rocks and its relationship to gas enrichment in yanchang area of ordos basin. *Unconv. Oil Gas* **2020**, *7*, 23–32, (In Chinese with English abstract).
7. Fu, J.H.; Wei, X.S.; Ren, J.F. Distribution and genesis of large-scale Upper Palaeozoic lithologic gas reservoirs on Yi-Shaan Slope. *Pet. Explor. Dev.* **2008**, *35*, 664–667, (In Chinese with English abstract). [CrossRef]
8. Dai, J.; Qin, S.; Hu, G.; NI, Y.; Gan, L.; Huang, S.; Hong, F. Major progress in the natural gas exploration and development in the past seven decades in China. *Pet. Explor. Dev.* **2019**, *46*, 1100–1110. [CrossRef]
9. Wang, S.J.; Li, D.H.; Li, J.Z.; Dong, D.Z.; Zhang, W.Z.; Ma, J. Exploration potential of shale gas in the Ordos Basin. *Nat. Gas. Ind.* **2011**, *31*, 40–46, (In Chinese with English abstract).
10. He, C.; Ji, L.; Su, A.; Wu, Y.; Zhang, M.; Zhou, S.; Li, J.; Hao, L.; Ma, Y. Source-rock evaluation and depositional environment of black shales in the Triassic Yanchang Formation, southern Ordos Basin, north-central China. *J. Pet. Sci. Eng.* **2019**, *173*, 899–911. [CrossRef]
11. Liu, C.Y.; Zhao, H.G.; Gui, X.J.; Yue, L.P.; Zhao, J.F.; Wang, J.Q. Space-Time coordinate of the evolution and reformation and mineralization response in ordos basin. *Acta Geol. Sin.* **2006**, *05*, 617–638, (In Chinese with English abstract).
12. Shi, W.; Dong, S.; Hu, J. Neotectonics around the Ordos Block, North China: A review and new insights. *Earth-Sci. Rev.* **2020**, *200*, 102969. [CrossRef]
13. Li, S.; Li, X.; Wang, G.; Liu, Y.; Wang, Z.; Wang, T.; Cao, X.; Guo, X.; Somerville, I.; Li, Y.; et al. Global Meso-Neoproterozoic plate reconstruction and formation mechanism for Precambrian basins: Constraints from three cratons in China. *Earth-Sci. Rev.* **2019**, *198*, 102946. [CrossRef]
14. Ju, Y.; Yu, K.; Wang, G.; Li, W.; Zhang, K.; Li, S.; Guo, L.; Sun, Y.; Feng, H.; Qiao, P.; et al. Coupling response of the Meso–Cenozoic differential evolution of the North China Craton to lithospheric structural transformation. *Earth-Sci. Rev.* **2021**, *223*, 103859. [CrossRef]
15. Li, W.H.; Chen, Q.; Li, Z.C.; Wang, R.G.; Wang, Y.; Ma, Y. Lithofacies palaeogeography of the Early Paleozoic in Ordos area. *J. Palaeogeogr.* **2012**, *14*, 85–100, (In Chinese with English abstract).
16. Guo, Y.H.; Liu, H.J.; Quan, B.; Wang, Z.C.; Qian, K. Late paleozoic sedimentary system and paleogeographic evolution of ordos area. *Acta Sedimentol. Sin.* **1998**, *16*, 44–51, (In Chinese with English abstract).
17. Xiao, H.P. *Depositional System and Favorable Reservoir of Shanxi Formation-He 8 Member in Ordos Basin*; China University of Geosciences: Beijing, China, 2020; (In Chinese with English abstract).
18. Meng, Q.-R.; Wu, G.-L.; Fan, L.-G.; Wei, H.-H. Tectonic evolution of early Mesozoic sedimentary basins in the North China block. *Earth-Sci. Rev.* **2019**, *190*, 416–438. [CrossRef]
19. Wang, Y.; Chen, S.Y.; Liang, H.Y.; Wang, J.; Li, T.B. Sedimentary facies and their evolution in the Upper Paleozoic of Baode rea, Ordos Basin. *Acta Sedimentol. Sin.* **2016**, *34*, 775–784, (In Chinese with English abstract).
20. Yu, X.H.; Wang, X.Z.; Wang, N.X.; Dan, X.; Zhou, J.S.; Han, X.Q.; Li, Y.L.; Du, Y.H.; Zhao, C.F. Sequence stratigraphic framework and sedimentary evolution characteristics of gas-bearing sandbody in the Upper Paleozoic in southeastern Ordos Basin. *J. Palaeogeogr.* **2017**, *19*, 935–954, (In Chinese with English abstract).
21. Feng, J.P.; Ou Yang, Z.J.; Chen, Q.H.; Li, W.H. Sedimentary characteristics of the upper Carboniferous in Ordos Basin and its adjacent areas. *J. Palaeogeogr.* **2021**, *23*, 53–64, (In Chinese with English abstract).
22. Ma, Y.; Li, W.H.; Zhang, Q.; Guo, Y.Q.; Yuan, Z.; Liao, Y. Sedimentary characteristics of the middle Permian in Ordos Basin and its adjacent areas. *J. Palaeogeogr.* **2021**, *23*, 81–92, (In Chinese with English abstract).
23. Guo, Y.Q.; Wang, M.X.; Guo, B.C.; Cai, Z.C.; Hui, L.; He, Z.Q.; Ma, Y.; Li, W.H.; Li, B.Q. Sedimentary system characteristics and paleographic evolution of Upper Paleozoic of northern west margin, Ordos Basin. *J. Northwest Univ.* **2020**, *50*, 93–104, (In Chinese with English abstract).
24. Li, W.H.; Zhang, Q.; Li, K.Y.; Chen, Q.; Guo, Y.Q.; Ma, Y.; Feng, J.P.; Zhang, D.F. Sedimentary evolution of the late Paleozoic in Ordos Basin and its adjacent areas. *J. Palaeogeogr.* **2021**, *23*, 39–52, (In Chinese with English abstract).
25. Ma, Y.; Li, W.H.; Wang, R.G.; Pang, J.G.; Wu, Y. Sedimentary facies and its evolution of the Upper Palaeozoic in Zizhou area of Ordos Basin. *Sci. Geol. Sin.* **2015**, *50*, 286–302, (In Chinese with English abstract).
26. Hao, L.; Ma, X.; Gao, W.; Ren, Z.; Tao, H.; Huang, W. Geochemical Characteristics of the Chang 7 Source Rocks of the Triassic Yanchang Formation in Ordos Basin, China: Implications for Organic Matter Accumulation and Shale Oil Potential. *Energies* **2022**, *15*, 7815. [CrossRef]
27. Li, Z.; Bao, Z.; Wei, Z.; Li, L.; Wang, H. Geochemical Features of Lacustrine Shales in the Upper Cretaceous Qingshankou Formation of Changling Sag, Songliao Basin, Northeast China. *Energies* **2022**, *15*, 6983. [CrossRef]
28. Chen, H.D.; Li, J.; Zhang, C.G.; Cheng, L.X.; Cheng, L.J. Discussion of sedimentary environment and its geological enlightenment of Shanxi formation in Ordos basin. *Acta Petrol. Sin.* **2011**, *27*, 2213–2229.
29. Li, M.; Gao, J. Basement faults and volcanic rock distributions in the Ordos Basin. *Sci. China Earth Sci.* **2010**, *53*, 1625–1633. [CrossRef]
30. Ma, X.; He, M.; Wang, J.; Gao, Y.; Zhu, D.; Liu, Y. Mine Strata Pressure Characteristics and Mechanisms in Gob-Side Entry Retention by Roof Cutting under Medium-Thick Coal Seam and Compound Roof Conditions. *Energies* **2018**, *11*, 2539. [CrossRef]
31. Peters, K.E.; Cassa, M.R. Applied source rock geochemistry. In *The Petroleum System-from Source to Trap, vol AAPG Memoir 60*; Magoon, L.B., Dow, W.G., Eds.; American Association of Petroleum Geologist: Tulsa, OK, USA, 1994; pp. 93–120.

32. Behar, F.; Beaumont, V.; De, B. Penteado, H.L. Rock-Eval 6 Technology: Performances and Developments. *Oil Gas Sci. Technol. Rev. l'IFP* **2001**, *56*, 111–134. [CrossRef]
33. Wu, L.Y.; Zhang, G.X. The application of pyrolysis technique in source rock research. *Acta Pet. Sin.* **1986**, *7*, 13–19, (In Chinese with English abstract).
34. Espitalie, J.; Deroo, G.; Marquis, F. La pyrolyse Rock-Eval et ses applications. Troisième partie. *Rev. L'inst. Français Pétrole.* **1986**, *41*, 73–89. [CrossRef]
35. Dembicki, H. Three common source rock evaluation errors made by geologists during prospect or play appraisals. *AAPG Bull.* **1993**, *93*, 341–356. [CrossRef]
36. El Kammar, M. Source-rock evaluation of the Dakhla Formation black shale in Gebel Duwi, Quseir area. *Egypt. J. Afr. Earth Sci.* **2015**, *104*, 19–26. [CrossRef]
37. Hatch, J.; Leventhal, J. Relationship between inferred redox potential of the depositional environment and geochemistry of the Upper Pennsylvanian (Missourian) Stark Shale Member of the Dennis Limestone, Wabaunsee County, Kansas, U.S.A. *Chem. Geol.* **1992**, *99*, 65–82. [CrossRef]
38. Baban, D.H. Sedimentary organic matter and source rock potential of the Paleocene Aaliji Formation in Qumar Oil Field, NE Iraq. *Arab. J. Geosci.* **2014**, *7*, 4733–4744. [CrossRef]
39. Welte, D.H.; Tissot, P.B. *Petroleum Formation and Occurrence*; Springer: New York, NY, USA, 1984.
40. Hunt, J.M. *Petroleum Geochemistry and Geology*; W.H, Freeman and Company: New York, NY, USA, 1995.
41. Jarvie, D.M.; Hill, R.J.; Ruble, T.E.; Pollastro, R.M. Unconventional shale-gas systems: The Mississippian Barnett Shale of north-central Texas as one model for thermogenic shale-gas assessment. *AAPG Bull.* **2007**, *91*, 475–499. [CrossRef]
42. Jia, J.; Liu, Z.; Bechtel, A.; Strobl, S.A.I.; Sun, P. Tectonic and climate control of oil shale deposition in the Upper Cretaceous Qingshankou Formation (Songliao Basin, NE China). *Int. J. Earth Sci.* **2013**, *102*, 1717–1734. [CrossRef]
43. Jones, B.; Manning, D.A.C. Comparison of geochemical indexes used for the interpretation of palaeoredox conditions in ancient mudstones. *Chem. Geol.* **1994**, *111*, 111–129. [CrossRef]
44. Borrok, D.M.; Yang, W.; Wei, M.; Mokhtari, M. Heterogeneity of the mineralogy and organic content of the Tuscaloosa Marine Shale. *Mar. Pet. Geol.* **2019**, *109*, 717–731. [CrossRef]
45. McLennan, S.M.; Hemming, S.; McDaniel, D.K.; Hanson, G.N. Geochemical approaches to sedimentation, provenance, and tectonics. In *Processes Controlling the Composition of Clastic Sediments*; Geological Society of America: McLean, VA, USA, 1993; pp. 21–40. [CrossRef]
46. Yang, W.L.; Li, Y.K.; Gao, R.Q.; Guo, Q.F. Type and evolution model of continental kerogen in the Songliao Basin. *Sci. China Chem.* **1982**, *25*, 304–317.
47. Ahmed, N.; Siddiqui, N.A.; Rahman, A.H.B.A.; Jamil, M.; Usman, M.; Sajid, Z.; Zaidi, F.K. Evaluation of hydrocarbon source rock potential: Deep marine shales of Belaga Formation of Late Cretaceous-Late Eocene, Sarawak, Malaysia. *J. King Saud Univ. Sci.* **2021**, *33*, 101268. [CrossRef]

Disclaimer/Publisher's Note: The statements, opinions and data contained in all publications are solely those of the individual author(s) and contributor(s) and not of MDPI and/or the editor(s). MDPI and/or the editor(s) disclaim responsibility for any injury to people or property resulting from any ideas, methods, instructions or products referred to in the content.